Dual-channel dispersionless slow light based on plasmon-induced transparency

Xiaoxiang Han

State Key Laboratory of Transient Optics and Photonics, Xi'an Institute of Optics and Precision Mechanics, Chinese Academy of Sciences, Xi'an 710119, China (hanxiaoxiang@opt.ac.cn)

Received 19 August 2013; revised 17 November 2013; accepted 19 November 2013; posted 3 December 2013 (Doc. ID 195999); published 23 December 2013

I have proposed a dual-channel dispersionless slow-light waveguide system based on plasmon-induced transparency. By appropriately tuning the stub depth, two transparency windows in the transmission spectrum can be achieved due to the destructive interference between the electromagnetic fields from the three stubs. Two flat bands can be achieved in the transparency windows, which have nearly constant group indices over the bandwidth of 2 THz. The analytical results show that the group velocity dispersion parameters of the two channels equal zero, which indicates that the incident pulse can be slowed down without distortion. The proposed plasmonic waveguide system can realize slow-light effect without pulse distortion, and thus can find important applications on slow-light systems, optical buffers, and all-optical signal processors in highly integrated optical circuits.

OCIS codes: (240.6680) Surface plasmons; (200.4490) Optical buffers; (130.3120) Integrated optics devices.

http://dx.doi.org/10.1364/AO.53.000009

1. Introduction

Slowing down the propagation speed of light to coherently trap and store optical pulses has drawn a lot of attention for its profound applications in optical communication and quantum information processing [1]. Slow light reveals its remarkable ability to reduce group velocity, which offers the possibility for time-domain processing of optical signals. Therefore, slow-light technology is vital to the development of all-optical packet-switched networks and photonic integrated circuits. Generally, slow light can be realized by two means: one is material dispersion [2,3], and the other is structural dispersion [4,5]. Many structures have been reported to realize slow-light effect [6–8] such as electromagnetically induced transparency (EIT), photonic crystal waveguide, and stimulated Raman scattering [9]. Among these approaches, EIT is a quantum interference phenomenon observed in three-level atomic systems. It features strong dispersion and slow-light propagation within the transparency window. Recently, researchers demonstrated that EIT-like spectrum can be realized in many classical structures [10–13]. For example, Lu *et al.* and Yanik *et al.* reported that EIT-like phenomenon can be realized in coupled resonators [12,14]. In addition, Gan and co-workers studied the slow-light mechanism of metallic grating structures, such as the rainbow trapping effect, on surface structures in different frequency domains [15,16].

Surface plasmon polaritons (SPPs) have shown the ability to overcome the diffraction limit of light in microchip-sized devices and thus are considered as one of the most promising candidates for integrated nanophotonic components. SPPs are waves that propagate along the surface of a conductor due to the interaction between the light waves and the free electrons of the conductor [17]. Plasmonic waveguides have numerous advantages: one is the better confinement of light with an acceptable propagation length and the other is, via altering the structural parameters, that their optical properties can be

1559-128X/14/010009-05$15.00/0

easily tailored [18,19]. In recent years, plasmonic waveguides have attracted great attention. Numerous devices based on plasmonic waveguides such as reflectors [20,21], the slow-light system [7], optical amplifiers [22], wavelength demultiplexers [23], absorbers [24], filters [25,26], couplers [27,28], sensors [19], and all-optical switching [29,30] have been investigated. Slow light can be easily observed close to the photonic bandgap (PBG) of the periodic structures. Recently, Wang *et al.* proposed a plasmonic graded grating waveguide system to realize slow-light effect and that structure performs well when it comes to the confinement of light [7]. However, the dispersion relation near the operating point of the PBG features a near parabolic characteristic, which means that a large group velocity dispersion (GVD) parameter may occur and result in severe pulse distortion. This may bring about the distortion to slow-light waves and cause serious information loss in highly integrated optical circuits. What's more, these devices are limited to a single-frequency at the PBG. These weaknesses severely confine the practical applications of the PBG structures. Last but not least, previous researches mainly focus on how to realize slow light on metal surface rather than the interior [31,32], this approach may result in large scattering loss due to its poor confinement of light. So it is highly important to investigate multiple-channel and dispersionless slow light.

In this paper, a dual-channel dispersionless slow-light plasmonic waveguide system is proposed. By using transmission line theory and finitedifference time-domain (FDTD) method, I theoretically and numerically investigated the proposed system based on the plasmon-induced transparency. Two transparency windows can be realized by appropriately tuning the stub depth. The transmission line results show that the two flat bands can be achieved and they have nearly constant group indices over the bandwidth of 2 THz. It has been found that the GVD of the proposed waveguide can reach zero, which indicates that the incident pulse can be slowed down without distortion. Given its high quality of drastically reducing the distortion of the incident pulse, the proposed slow-light system can find significant applications on optical buffers and all-optical signal processors in highly integrated optical circuits.

2. Structure Model and Theory

The schematic diagram of the proposed plasmonic waveguide system is shown in Fig. 1. There are three stubs that side coupled to the metal–insulator–metal (MIM) waveguide in each unit cell. When a TM-polarized plane wave is coupled into the waveguide, SPP waves can be excited at the metal-insulator interfaces and confined in the insulator layer. The metal in my structure is selected as silver, whose frequency-dependent relative permittivity is characterized by the Drude model [33,34]:

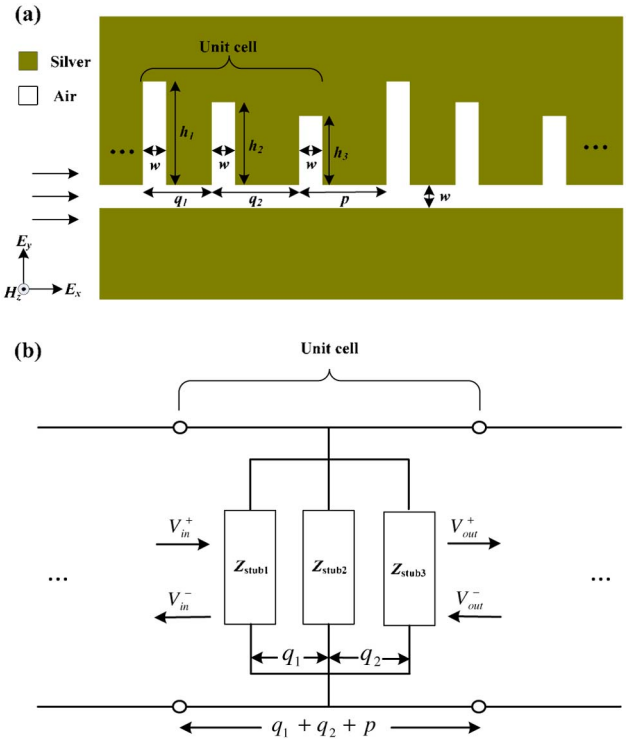

Fig. 1. (a) Schematic of the MIM plasmonic waveguide system: w, the width of the waveguide and stubs; $q_1 + q_2 + p$, the period of each unit cell; q, the distance between the stubs in a unit cell; h, the stub depth. The light vertically illuminates the structure from the left side. (b) Equivalent circuits of the proposed plasmonic waveguide system. Z_{stub1}, Z_{stub2}, and Z_{stub3} represent the effective impedances of the first, second, and third stubs, respectively.

$$\varepsilon_m(\omega) = \varepsilon_\infty - \frac{\omega_p^2}{\omega(\omega + i\gamma)}. \quad (1)$$

Where $\varepsilon_\infty = 3.7$ is the dielectric constant at infinite angular frequency. ω_p is 9.1 eV and stands for the bulk plasma frequency, which represents the natural frequency of the oscillations of free conduction electrons. γ is 0.018 eV and represents the damping frequency of the oscillations. ω is the angular frequency of the incident wave in vacuum [35].

Here, an improved transmission model [36] is used to account for the transmission and dispersion properties of the system. According to the transmission line theory, the plasmonic waveguide system is equivalent to a parallel connection of an infinite transmission line and a serial finite transmission line. The infinite transmission line is characterized with the impedance of $Z_{\mathrm{MIM}} = \beta_0 w/\omega\varepsilon_0\varepsilon_{\mathrm{air}}$ (representing the MIM waveguide) and the serial finite transmission line is characterized with the impedance Z_S terminated by a load Z_L (representing the stub). For simplicity, the stub section can be replaced by an effective impedance described by $Z_{\mathrm{stub}} = Z_S(Z_L - iZ_S\tan(\beta_S h))/(Z_S - iZ_L\tan(\beta_S h))$, where $Z_S = \beta_S w/\omega\varepsilon_0\varepsilon_{\mathrm{air}}$ and $Z_L = (\varepsilon_m/\varepsilon_{\mathrm{air}})^{1/2} Z_S$. $\beta_0(\beta_S)$ is the propagation constant of the fundamental mode in the MIM waveguide (stub), h is the depth of the stub. Thus, the transmission of plasmonic

waveguide system can be given by $T = A(p/2)B(Z_{stub1})A(q_1)B(Z_{stub2})A(q_2)B(Z_{stub3})A(p/2)$, where the expression of $A(x)$ and $B(\text{stub})$ can be found in [31,36]. The dispersion relation between the frequency and Bloch wave number $K = \alpha + i\beta$ of the entire system can be obtained as

$$\cos h(K(p + q_1 + q_2)) = \frac{1}{2}(T(1,1) + T(2,2)). \quad (2)$$

3. Numerical Results and Analysis

First of all, I investigate the transmission properties of the plasmonic waveguide side-coupled to one unit cell by using transmission line theory [37,38]. As shown in Fig. 2(a), there are two transmission peaks at the frequencies of 283 and 310 THz in a wide low-transmission band. There are three transmission dips at the frequencies of 273, 297, and 322 THz, corresponding to the resonant frequencies of the three stubs. The transmission of the two transmitted peaks is about 0.4, which is much higher than that in [39]. In addition, the propagation loss of one unit cell is about -2.154×10^4 dB/cm. Though the ohm loss of metal can not be ignored, it can be perfectly compensated by introducing gain media into the proposed slow-light system [9]. The dispersion relationship of the two channels is shown in Fig. 2(b). It can be seen that two flat bands can be found, which implies that dual-channel slow-light effect can be realized in the proposed plasmonic waveguide. Especially, the dispersion curves are flat, which indicates that nearly constant group index can be obtained. To confirm this, the FDTD method is employed to calculate the transmission spectrum of one periodic unit. It is found that the simulations agree well with the transmission line results. Figures 2(c) and 2(d) clearly depict the field distributions of channels 1 and 2, respectively. That is to say, the channel 1 (2) is attributed to the destructive interference of the SPP waves reflected from the first (second) and second (third) stubs.

Since the stubs side-coupled to the plasmonic waveguide act as high-efficient reflectors, the SPP waves can be reflected repeatedly between the two stub resonators with high reflectivity, forming a Fabry–Perot resonator [40,41], as shown in Figs. 2(c) and 2(d). The different stub depths result in different resonance wavelengths in the transmission spectra. The distance between the stubs determines the phase-difference between the reflected SPP waves. So when appropriately tuning q_1, q_2, h_1, h_2, and h_3, I can obtain two very narrow transparency windows due to the destructive interference between the reflected SPP waves. There is no EIT-like peak resulting from the interaction between the first and third stubs. This is because in my slow-light system, the depths of the first and third stubs are 580 and 485 nm, respectively. The difference of these two stub depths is as large as 95 nm, which means that the difference of the corresponding resonance wavelengths is also very large. Thus, the reflected lights from the first and third stubs have the very large detuning. There is no destructive interference between the first and third stubs. The wavelength shifts to long wavelength with the increase of stub depths (i.e., h_1, h_2, and h_3) [42]. The transmission of the two channels changes periodically with the variation of the distance between the stubs (i.e., q_1 and q_2),

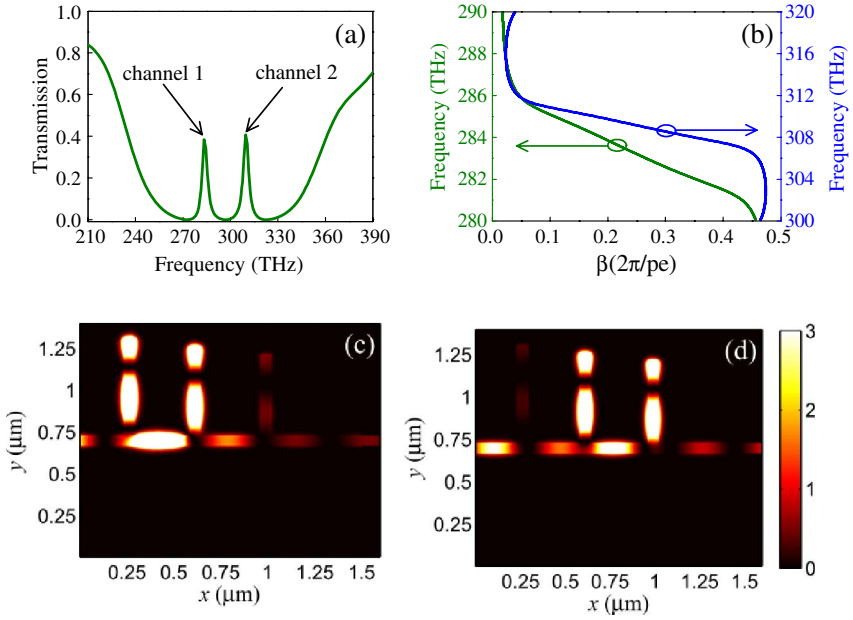

Fig. 2. (a) Transmission spectrum from the transmission line theory with $q_1 = 350$ nm, $q_2 = 380$ nm, $p = 300$ nm, $h_1 = 580$ nm, $h_2 = 530$ nm, $h_3 = 485$ nm, and $w = 50$ nm. (b) Dispersion curves calculated by using transmission line theory. The parameter $pe = q_1 + q_2 + p$. The green and blue lines correspond to channel 1 and channel 2, respectively. (c)–(d) Field distributions of $|\text{Hz}|^2$ at the induced-transparency frequencies of 283 and 310 THz, respectively.

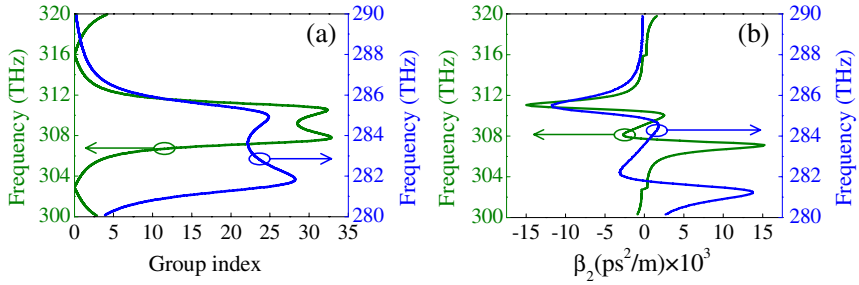

Fig. 3. (a) Group indices of SPP waves for the two channels as a function of frequency. (b) Second-order dispersion parameters of the two channels. The blue and green lines correspond to channel 1 and channel 2, respectively.

which determines the phase-difference between the reflected SPP waves. When the phase-difference between the reflected SPP wares is $2n\pi$ (n is the integer number), the transmission of the two channels reaches the peak. When the phase-difference is $2(n+1)\pi$, the transmission is minimal. It should be noted that when more stubs are cascaded in the MIM waveguide, and the stub depth and distance between the stubs are appropriately adjusted, the destructive interference between the SPP waves reflected from the stubs can result in multiple narrow transparency windows, and more EIT-like transmission peaks can be obtained.

Successively, I calculate the dispersion relationship and the corresponding group indices at different frequencies with the stub depths h_1, h_2, and h_3. In the calculations, the group index is defined as

$$n_g = c/v_g = cd\beta/d\omega. \tag{3}$$

The corresponding group index is shown in Fig. 3(a). Generally, one considers n_g to be constant within a $\pm 10\%$ range. By numerically investigating the dual-channel slow-light plasmonic waveguide system, I obtain a flat bandwidth over 2 THz in the sense of the above criterion. In other words, I achieve a very flat dispersion curve with nearly constant group index. The higher-order dispersions of SPP waves in the proposed plasmonic waveguide system are also calculated. Here, the second-order dispersion parameters are characterized by $\beta_2 = d^2k/d\omega^2$ [43]. As shown in Fig. 3(b), the GVD parameters near the transmission peak of the two channels are equal to zero. It means that an incident pulse centered at the frequencies of the transmission peaks will experience almost no distortion. In conclusion, the incident pulse can be slowed down without distortion, due to the nearly constant group index and the zero GVD. Moreover, I calculate the group index-bandwidth product (GBP). The GBP is one of the standards to evaluate the slow-light performance and it is defined as GBP $\approx \tilde{n}_g(\Delta\omega/\omega)$ [4,13], here $\tilde{n}_g$ represents the average group index given as

$$\tilde{n}_g = \int_{\omega_0}^{\omega_0+\Delta\omega} n_g(\omega) \times \mathrm{d}\omega/\Delta\omega. \tag{4}$$

In the proposed slow-light system, the GBP is 0.156 and 0.184 for channel 1 and channel 2, respectively.

As we know, the dispersive effect is one of the intrinsic features for the periodic structure. A periodic structure will exhibit dispersive effect even if it is fabricated in a nondispersive medium. The above dispersive properties are essentially attributed to the periodic structures, which is the so-called structural dispersion. When appropriately tuning the geometrical parameters, the grating-induced dispersion may compensate the dispersion of the metal. In this case, the material dispersion of the silver is counterbalanced by the structural dispersion of the dual-channel slow-light waveguide system. Therefore, a low GVD parameter can be achieved and I can obtain the distortionless slow light.

4. Conclusion

I have proposed and numerically investigated a plasmonic slow-light waveguide system by using the transmission line theory and the FDTD method. The transmission results show that plasmon-induced transparency can be achieved. The transmission and dispersion properties are investigated by the transmission line theory. It is found that two flat dispersion curves with nearly constant group indices over a bandwidth of 2 THz can be obtained. Moreover, the GVD parameters can reach zero, implying that the incident pulse can be slowed down without distortion. So the proposed plasmonic waveguide system may find potential applications on slow-light systems, optical buffers, and all-optical signal processors in highly integrated circuits.

This work was supported by the National Natural Science Foundation of China under Grants 61223007 and 11204368.

References

1. M. F. Yanik and S. Fan, "Stopping light all optically," Phys. Rev. Lett. **92**, 083901 (2004).
2. L. V. Hau, S. E. Harris, Z. Dutton, and C. H. Behroozi, "Light speed reduction to 17 metres per second in an ultracold atomic gas," Nature **397**, 594–598 (1999).
3. A. V. Turukhin, V. S. Sudarshanam, M. S. Shahriar, J. A. Musser, B. S. Ham, and P. R. Hemmer, "Observation of ultraslow and stored light pulses in a solid," Phys. Rev. Lett. **88**, 0236021 (2002).
4. T. Baba, "Slow light in photonic crystals," Nat. Photonics **2**, 465–473 (2008).

5. Y. A. Vlasov, M. O'Boyle, H. F. Hamann, and S. J. McNab, "Active control of slow light on a chip with photonic crystal waveguides," Nature **438**, 65–69 (2005).
6. L. Yang, C. Min, and G. Veronis, "Guided subwavelength slow-light mode supported by a plasmonic waveguide system," Opt. Lett. **35**, 4184–4186 (2010).
7. G. Wang, H. Lu, and X. Liu, "Trapping of surface plasmon waves in graded grating waveguide system," Appl. Phys. Lett. **101**, 013111 (2012).
8. G. Wang, H. Lu, and X. Liu, "Gain-assisted trapping of light in tapered plasmonic waveguide," Opt. Lett. **38**, 558–560 (2013).
9. M. Sandtke and L. Kuipers, "Slow guided surface plasmons at telecom frequencies," Nat. Photonics **1**, 573–576 (2007).
10. R. Kekatpure, E. S. Barnard, W. Cai, and M. L. Brongersma, "Phase-coupled plasmon-induced transparency," Phys. Rev. Lett. **104**, 243902 (2010).
11. H. Lu, X. Liu, D. Mao, Y. Gong, and G. Wang, "Induced transparency in nanoscale plasmonic resonator systems," Opt. Lett. **36**, 3233–3235 (2011).
12. H. Lu, X. Liu, and D. Mao, "Plasmonic analog of electromagnetically induced transparency in multi-nanoresonator-coupled waveguide systems," Phys. Rev. A **85**, 053803 (2012).
13. A. Ishikawa, R. F. Oulton, T. Zentgraf, and X. Zhang, "Slow-light dispersion by transparent waveguide plasmon polaritons," Phys. Rev. B **85**, 155108 (2012).
14. M. F. Yanik, W. Suh, Z. Wang, and S. Fan, "Stopping light in a waveguide with an all-optical analog of electromagnetically induced transparency," Phys. Rev. Lett. **93**, 233903 (2004).
15. Q. Gan, Y. J. Ding, and F. J. Bartoli, "'Rainbow trapping and releasing at telecommunication wavelengths," Phys. Rev. Lett. **102**, 056801 (2009).
16. Q. Gan and F. J. Bartoli, "Surface dispersion engineering of planar plasmonic chirped grating for complete visible rainbow trapping," Appl. Phys. Lett. **98**, 251103 (2011).
17. W. L. Barnes, A. Dereux, and T. W. Ebbesen, "Surface plasmon subwavelength optics," Nature **424**, 824–830 (2003).
18. D. K. Gramotnev and S. I. Bozhevolnyi, "Plasmonics beyond the diffraction limit," Nat. Photonics **4**, 83–91 (2010).
19. H. Lu, X. M. Liu, D. Mao, L. Wang, and Y. Gong, "Tunable band-pass plasmonic waveguide filters with nanodisk resonators," Opt. Express **18**, 17922–17927 (2010).
20. Z. Han, E. Forsberg, and S. He, "Surface plasmon Bragg gratings formed in metal-insulator-metal waveguides," IEEE Photon. Technol. Lett. **19**, 91–93 (2007).
21. B. Wang and G. P. Wang, "Plasmon Bragg reflectors and nanocavities on flat metallic surfaces," Appl. Phys. Lett. **87**, 013107 (2005).
22. I. De Leon and P. Berini, "Amplification of long-range surface plasmons by a dipolar gain medium," Nat. Photonics **4**, 382–387 (2010).
23. H. Lu, X. Liu, Y. Gong, D. Mao, and L. Wang, "Enhancement of transmission efficiency of nanoplasmonic wavelength demultiplexer based on channel drop filters and reflection nanocavities," Opt. Express **19**, 12885–12890 (2011).
24. Y. Gong, X. Liu, L. Wang, H. Lu, and G. Wang, "Multiple responses of TPP-assisted near-perfect absorption in metal/Fibonacci quasiperiodic photonic crystal," Opt. Express **19**, 9759–9769 (2011).
25. H. Lu, X. Liu, Y. Gong, L. Wang, and D. Mao, "Multi-channel plasmonic waveguide filters with disk-shaped nanocavities," Opt. Commun. **284**, 2613–2616 (2011).
26. Y. Gong, X. Liu, and L. Wang, "High-channel-count plasmonic filter with the metal–insulator–metal Fibonacci-sequence gratings," Opt. Lett. **35**, 285–287 (2010).
27. G. Veronis and S. Fan, "Theoretical investigation of compact couplers between dielectric slab waveguides and two-dimensional metal-dielectric-metal plasmonic waveguides," Opt. Express **15**, 1211–1221 (2007).
28. R. A. Wahsheh, Z. Lu, and M. A. Abushagur, "Nanoplasmonic couplers and splitters," Opt. Express **17**, 19033–19040 (2009).
29. H. Lu, X. Liu, L. Wang, Y. Gong, and D. Mao, "Ultrafast all-optical switching in nanoplasmonic waveguide with Kerr nonlinear resonator," Opt. Express **19**, 2910–2915 (2011).
30. G. Wang, H. Lu, X. Liu, and Y. Gong, "Numerical investigation of an all-optical switch in a graded nonlinear plasmonic grating," Nanotechnology **23**, 444009 (2012).
31. S. He, Y. He, and Y. Jin, "Revealing the truth about 'trapped rainbow' storage of light in metamaterials," Sci. Reports **2**, 583 (2012).
32. Q. Gan, Y. Gao, K. Wagner, D. Vezenov, Y. J. Ding, and F. J. Bartoli, "Experimental verification of the "rainbow" trapping effect in adiabatic plasmonic gratings," Proc. Natl. Acad. Sci. USA **108**, 5169–5173 (2011).
33. G. Wang, H. Lu, X. Liu, D. Mao, and L. Duan, "Tunable multi-channel wavelength demultiplexer based on MIM plasmonic nanodisk resonators at telecommunication regime," Opt. Express **19**, 3513–3518 (2011).
34. G. Wang, H. Lu, X. Liu, Y. Gong, and L. Wang, "Optical bistability in metal-insulator-metal plasmonic waveguide with nanodisk resonator containing Kerr nonlinear medium," Appl. Opt. **50**, 5287–5290 (2011).
35. J. Park, H. Kim, and B. Lee, "High order plasmonic Bragg reflection in the metal-insulator-metal waveguide Bragg grating," Opt. Express **16**, 413–425 (2008).
36. A. Pannipitiya, I. D. Rukhlenko, M. Premaratne, H. T. Hattori, and G. P. Agrawal, "Improved transmission model for metal-dielectric-metal plasmonic waveguides with stub structures," Opt. Express **18**, 6191–6204 (2010).
37. G. Veronis and S. Fan, "Bends and splitters in metal-dielectric-metal subwavelength plasmonic waveguides," Appl. Phys. Lett. **87**, 131102 (2005).
38. J. Liu, G. Fang, H. Zhao, Y. Zhang, and S. Liu, "Surface plasmon reflector based on serial stub structure," Opt. Express **17**, 20134–20139 (2009).
39. L. Chen, G. Wang, Q. Gan, and F. J. Bartoli, "Trapping of surface-plasmon ploaritons in a graded Bragg structure: Frequency-dependent spatially separated localization of the visible spectrum modes," Phys. Rev. B **80**, 161106 (2009).
40. H. Lu, X. Liu, Y. Gong, D. Mao, and G. Wang, "Analysis of nanoplasmonic wavelength demultiplexing based on metal-insulator-metal waveguide," J. Opt. Soc. Am. B **28**, 1616–1621 (2011).
41. J. Chen, C. Wang, R. Zhang, and J. Xiao, "Multiple plasmon-induced transparencies in coupled-resonator systems," Opt. Lett. **37**, 5133–5135 (2012).
42. X. Lin and X. Huang, "Tooth-shaped plasmonic waveguide filters with nanometeric sizes," Opt. Lett. **33**, 2874–2876 (2008).
43. G. Wang, H. Lu, and X. Liu, "Dispersionless slow light in MIM waveguide based on a plasmonic analogue of electromagnetically induced transparency," Opt. Express **20**, 20902–20907 (2012).